

TTI/VTI anisotropy parameters estimation by focusing analysis, Part I: theory

Jun Cai*, Yang He, Zhiming Li, Bin Wang, Manhong Guo

TGS-NOPEC Geophysical Company, 2500 CityWest Blvd. Suite 2000, Houston, TX 77042, USA

Summary

Time domain and depth domain focusing operators are introduced to estimate anisotropic parameters. The fully automated time domain focusing operator to derive anisotropy model for depth migration method is proposed and developed. The approach can be used for both surface seismic data and VSP seismic data.

Introduction

Prestack depth migration and velocity model analysis for isotropic media have been widely used to image the complex structure area. In order to improve the positioning accuracy and the image quality, seismic anisotropy is needed in most places of the world. The challenge is to estimate and build the anisotropy model for depth migration.

The majority of anisotropy model building for depth migration works have been focused on anisotropic tomography to flatten the common imaging gathers (CIG) (Zhou et al., 2003, Zhou et al., 2004; Yuan et al. 2006).

For isotropic velocity analysis, Delphi proposed the common focus-point (CFP) approach (Berkhout 1997), which splits the migration velocity analysis into two steps, first determined the migration operator from the seismic data, and then translated the operator into a velocity model. Recently they published the work to construct the two-way traveltime common focusing operator from two one-way traveltimes by using one-way traveltime common focusing operator (Verschuur and Marhfoel, 2009).

We propose focusing operator concept, and apply focusing operators to the CIG to perform the anisotropy parameter estimation, which is somewhat similar to Delphi's CFP concept. Instead splitting the analysis process into two independent steps like Delphi's approach, we implement it in one step, which the anisotropy models is part of the calculation to construct the focusing operator. In this study, we assume the normal velocity, v_0 , and the anisotropy symmetry axis angles (dipping angle, θ , and azimuth angle, ϕ) are known for TTI media. The method can be extended to solve v_0 , θ , and ϕ by adding three more unknowns.

Focusing operators in time domain

In order to construct the focusing operator, we take the zero-offset migration imaging point in CIG as focal point.

To make the program fully automated, we perform demigration for the CIG gather to get the correct focusing operator in time domain. The focusing operator will produce a resolution higher than picking travel times in time domain. The demigration approach thus improves the accuracy of the anisotropy parameter estimation. It also allows the initial model to be either isotropic or anisotropic. In turn, this technique can be used to build the anisotropy model from initial check shot or used as a fine tune tool to adjust the existing anisotropy model. Then we can construct the calculated focusing operators for current anisotropy model by ray tracing from the focal point.

For VTI media, assuming the vertical velocity, v_0 , is known. Figure 1A shows the one-way traveltime VTI focusing operators, which are suitable for estimating anisotropy from walk-away VSP's first arrival data, for constant velocity ($v=2500\text{m/s}$) anisotropy models. The red curve is the true focusing operator for the correct anisotropy model ($\epsilon=0.1$, $\delta=0.05$). The orange curve is the focusing operator for larger anisotropy model ($\epsilon=0.2$, $\delta=0.1$). The green curve is the focusing operator for isotropic model (smaller anisotropy, $\epsilon=0$, $\delta=0$).

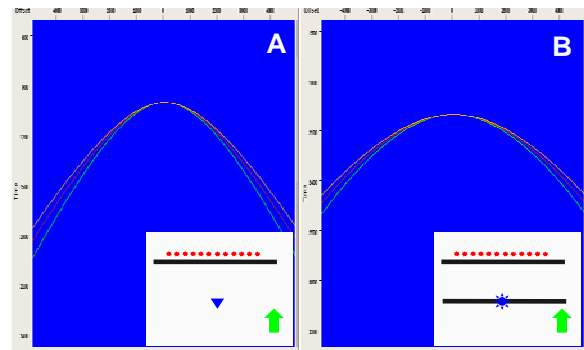


Figure 1: VTI focusing operators. The green arrows show the anisotropy symmetry axis. (A) One-way traveltime VTI focusing operators. (B) Two-way traveltime VTI focusing operators.

Figure 1B shows the two-way traveltime VTI focusing operators, which are suitable for estimating anisotropy from surface reflection data for constant velocity ($v=2500\text{m/s}$) anisotropy models. The red curve is the true focusing operator for the correct anisotropy model ($\epsilon=0.1$, $\delta=0.05$). The orange curve is the focusing operator for larger anisotropy model ($\epsilon=0.2$, $\delta=0.1$). The green curve is the

TTI/VTI anisotropy parameters estimation by focusing analysis, Part I: theory

focusing operator for isotropy model (smaller anisotropy, $\epsilon=0, \delta=0$).

For TTI media, assuming the normal velocity, v_0 , and dipping angle, θ (2D), are known. Figure 2A shows the one-way traveltime TTI focusing operators, for constant velocity ($v=2500\text{m/s}$) anisotropy models. The red curve is the true focusing operator for the correct anisotropy model ($\epsilon=0.1, \delta=0.05, \theta=-45^\circ$). The orange curve is the focusing operator for larger anisotropy model ($\epsilon=0.2, \delta=0.1, \theta=-45^\circ$). The green curve is the focusing operator for isotropy model (smaller anisotropy, $\epsilon=0, \delta=0, \theta=-45^\circ$). We can see all three curves are almost overlap following the anisotropy symmetry axis (the green arrow); and the apexes are shifted between three cases.

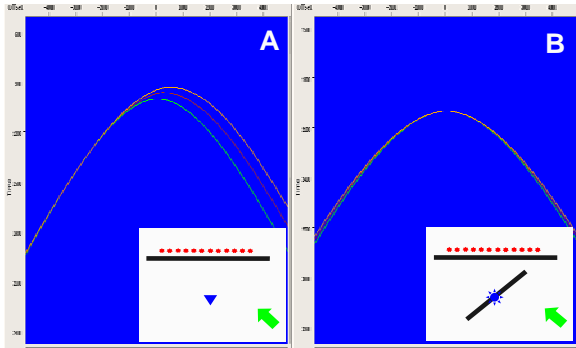


Figure 2: TTI focusing operators. The green arrows show the anisotropy symmetry axis. (A) One-way traveltime TTI focusing operators. (B) Two-way traveltime TTI focusing operators.

Figure 2B shows the two-way traveltime TTI focusing operators for constant velocity ($v=2500\text{m/s}$) anisotropy models. The red curve is the true focusing operator for the correct anisotropy model ($\epsilon=0.1, \delta=0.05, \theta=-45^\circ$). The orange curve is the focusing operator for larger anisotropy model ($\epsilon=, \delta=, \theta=-45^\circ$). The green curve is the focusing operator for isotropy model ($\epsilon=0, \delta=0, \theta=-45^\circ$).

From Figure 1 and Figure 2, we can see the focusing operators for VSP provides the best indication to identify the VTI and TTI media.

Automatically search VTI and TTI parameters

To search the correct anisotropy parameters, we define the objective function as

$$\Delta = \min \|f_{cal}(\epsilon_{cal}, \delta_{cal}, x_f) - f_{true}(\epsilon_{true}, \delta_{true}, x_f)\|$$

where f_{cal} is the calculated the focus operator, which is the function of updated anisotropy parameters, ϵ_{cal} and δ_{cal} , and the focal point x_f . f_{true} is the true focus operator, which is the function of true anisotropy parameters, ϵ_{true} and δ_{true} , and the focal point x_f . We can use either $L1$ or $L2$ criteria. For this study, we use $L1$, since it is less sensitive to the outliers. We can get the f_{true} with sub-sample accuracy by demigrating the CIG with its corresponding migration (isotropy or anisotropy) models.

Figure 3 shows the VTI anisotropy estimation for a flat layer constant velocity model ($v=2500\text{m/s}$). First we migrated the input synthetic data (Figure 3A), then auto-pick the curve in the CIG (Figure 3B) for demigration to calculate the true focusing operator. The $L1$ object function is calculated and shown in Figure 3C. The final results are shown in Figure 3D.

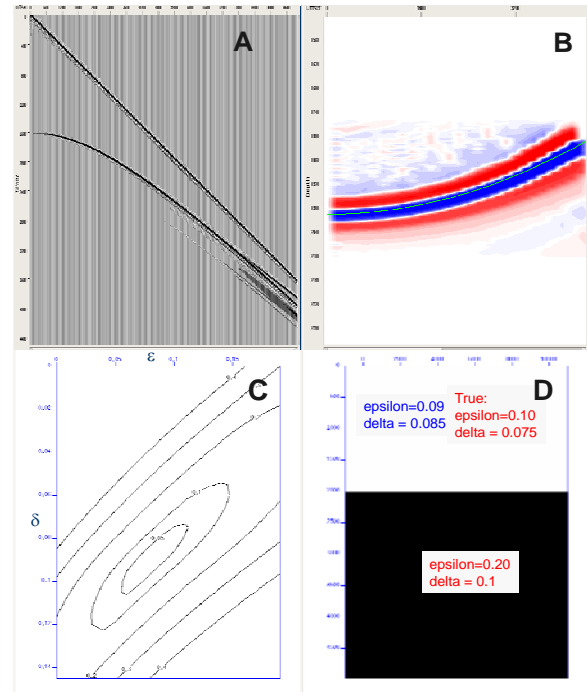


Figure 3: (A) VTI synthetic data. (B) CIG, the green curve is the curve used for demigration. (C) The objective function contour as function of ϵ and δ . (D) The true and estimated anisotropy parameters.

Figure 4 shows the TTI anisotropy estimation for two layer gradient velocity model (Figure 4A). The true and estimated anisotropy models are shown in Figure 4B.

TTI/VTI anisotropy parameters estimation by focusing analysis, Part I: theory

Figure 4C shows the objective function contours for top and bottom layers. Figure 4D shows the true and calculated focusing operators before and after estimation for both layers. One observation is that the estimated anisotropy for bottom layer contains more errors than the first layer. It could be couple factors,

1. The accumulated error from first layer. The smaller estimated ϵ in the first layer could lead to larger ϵ in the second layer.
2. Less time difference in the focusing operators. We can see it by comparing Figure 6E with Figure 6G.
3. Another way to look at item 2 is in the objective function contour plots, second layer has less well defined contours comparing with first layer.

Focusing operators in depth domain

The focusing operator in depth domain can also be constructed. First we calculate the correct focusing operators in time domain. Then we perform migration for different offsets by using one of the candidate anisotropy models. We will use the one layer TTI media to demonstrate the concept. Figure 5 shows the partial migration imaging for all the offsets and different anisotropy models.

We stack along the offsets direction, and define it as the focusing operator in depth domain. When the anisotropy is larger than the true value, the focusing operator is spread out along the wave front (Figure 6A). When the anisotropy parameters are correct, we will get the best focusing (Figure 7A). When the anisotropy is smaller (isotropy) than the true value, the focusing operator is spread in along the wave front (Figure 8A). Only when the true model is used the wavelet has zero phase.

In Figure 5, if we cut along the offset direction at the central location vertically, we will obtain the conventional CIG (Figure 6C, Figure 7C, and Figure 8C). If we cut along the anisotropy symmetry axis, then we will get well defined events and residual curves (Figure 6B, Figure 7B, and Figure 8B). In the TTI tomography approach, we normally using the dip information and project the CIG gather's moveout to the symmetry plane. These figures show that there are more to gain if performing the TTI analysis within the plane defined by the anisotropy symmetry axis.

Conclusions

Focusing operators in both time domain and depth domain are introduced. Anisotropy parameter can be obtained by focusing analysis for both VTI and TTI media. During the processing, the object is to find the minimum object function between the true focusing operator and calculated

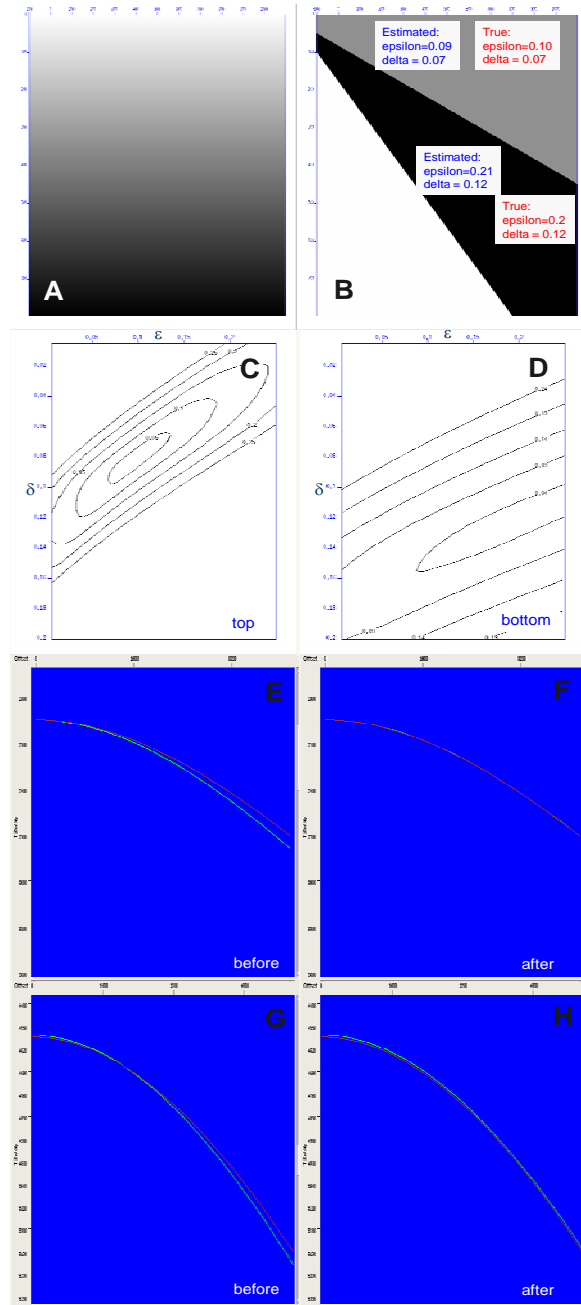


Figure 4: TTI gradient velocity model (A); true and estimated anisotropy parameters (B). (C) and (D) are the objective functions for top and bottom layers. E, F, G, and H are the initial and updated focusing operators for top layer (E and F) and bottom layer (G and H). Red curves are correct focusing operators; green curves are the calculated focusing operators.

TTI/VTI anisotropy parameters estimation by focusing analysis, Part I: theory

focusing operator. It can be used for both VSP data and surface reflection seismic data. The algorithm is fully automated. The synthetic data shows the effectiveness of the algorithm.

Acknowledgments

Authors like to thank their colleagues Kwangjin Yoon, Eric Nessler, and Tefera Eshete for their valuable contributions during the project. And thanks to TGS-NOPEC for their support and the release of material for publication.

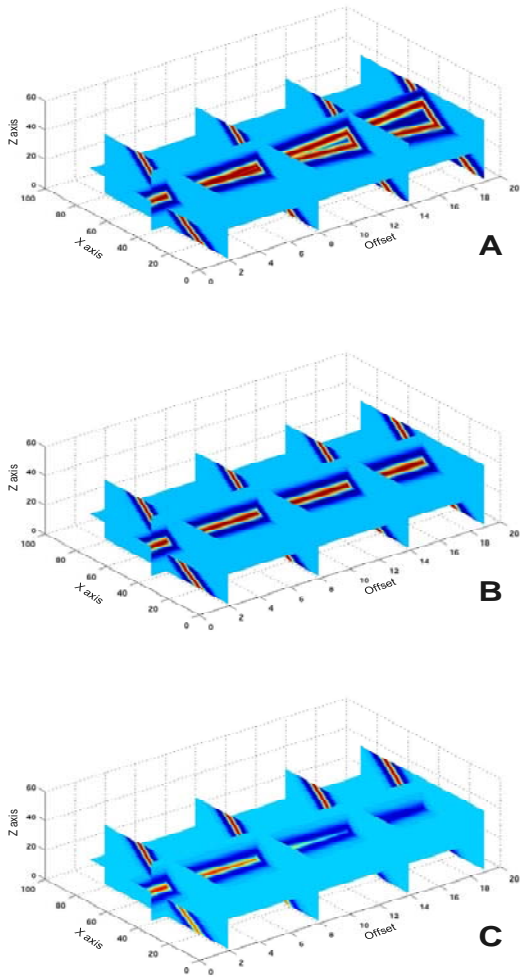


Figure 5: Partial migration to construct the focusing operators in depth domain for TTI media. (A) Isotropic media ($\epsilon=0$, $\delta=0$, $\theta=45^\circ$). (B) True anisotropy ($\epsilon=0.1$, $\delta=0.05$, $\theta=45^\circ$). (C) Larger anisotropy ($\epsilon=0.2$, $\delta=0.1$, $\theta=45^\circ$).

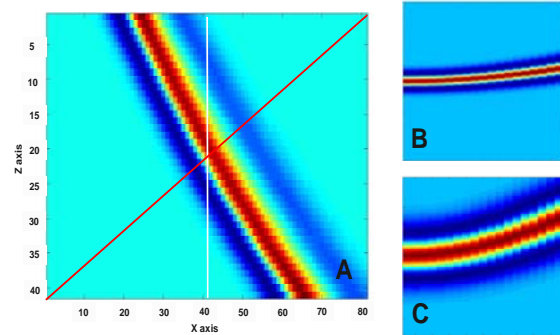


Figure 6: (A) TTI focusing operator in depth domain for isotropy (smaller anisotropy parameter, Figure 5C). (B) Cut along symmetry axis. (C) Cut along vertical equals to CIG.

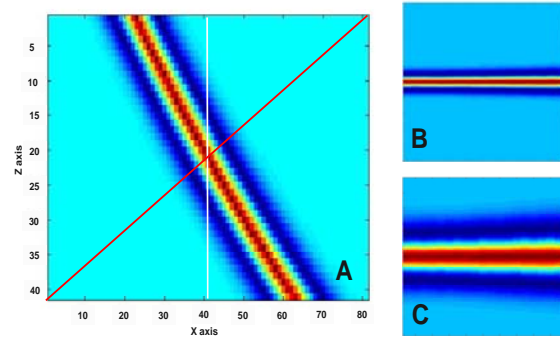


Figure 7: (A) TTI focusing operator in depth domain for true anisotropy parameter (Figure 5B). (B) Cut along symmetry axis. (C) Cut along vertical equals to CIG.

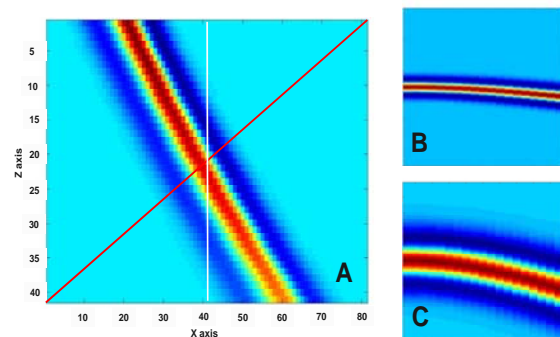


Figure 8: (A) TTI focusing operator in depth domain for larger anisotropy parameter (Figure 5A). (B) Cut along symmetry axis. (C) Cut along vertical equals to CIG.

EDITED REFERENCES

Note: This reference list is a copy-edited version of the reference list submitted by the author. Reference lists for the 2009 SEG Technical Program Expanded Abstracts have been copy edited so that references provided with the online metadata for each paper will achieve a high degree of linking to cited sources that appear on the Web.

REFERENCES

- Berkhout, A. J., 1997, Pushing the limits of seismic imaging, Part II: Integration of prestack migration, velocity estimation and AVO analysis: *Geophysics*, **62**, 954–969.
- Verschuur, E., and B. E. Marhfoul, 2009, Estimation of 2D and 3D near surface datuming operators by global optimization: DELPHI Acquisition and Preprocessing Project Volume XIII, Annual Report January 2009, Chapter 10.
- Yuan, J., X. Ma, S. Lin, and D. Lowrey, 2006, P-wave tomographic velocity updating in 3D inhomogeneous VTI media: 76th Annual International Meeting, SEG, Expanded Abstracts, 3368–3372.
- Zhou, H., D. Pham, S. Gray, and B. Wang, 2003, 3-D tomographic velocity analysis in transversely isotropic media: 73rd Annual International Meeting, SEG, Expanded Abstracts, 650–654.
- , 2004, Tomographic velocity analysis in strong anisotropic TTI media: 74th Annual International Meeting, SEG, Expanded Abstracts, 2347–2351.